THE FASEB JOURNAL • RESEARCH • www.fasebj.org

Phenotypic transformation of intimal and adventitial lymphatics in atherosclerosis: a regulatory role for soluble VEGF receptor 2

Mahdi Taher,[*,†,‡,§,¶] Shintaro Nakao,[*,†,‡,§] Souska Zandi,[*,†,‡,§] Mark I. Melhorn,[*,†,‡,§] K. C. Hayes,[‖] and Ali Hafezi-Moghadam[*,†,‡,§,1]

[*]Center for Excellence in Functional and Molecular Imaging, Brigham and Women's Hospital, Boston, Massachusetts, USA; [†]Department of Radiology and [‡]Angiogenesis Laboratory, Massachusetts Eye and Ear Infirmary, and [§]Department of Ophthalmology, Harvard Medical School, Boston, Massachusetts, USA; [¶]Institute of Biochemistry, Charité University Medical Center, Berlin, Germany; and [‖]Department of Biology, Brandeis University, Waltham, Massachusetts, USA

ABSTRACT: The role of lymphatics in atherosclerosis is not yet understood. Here, we investigate lymphatic growth dynamics and marker expression in atherosclerosis in apolipoprotein E–deficient ($apoE^{-/-}$) mice. The prolymphangiogenic growth factor, VEGF-C, was elevated in atherosclerotic aortic walls. Despite increased VEGF-C, we found that adventitial lymphatics regress during the course of formation of atherosclerosis ($P < 0.01$). Similar to lymphatic regression, the number of lymphatic vessel endothelial hyaluronan receptor 1 (LYVE-1$^+$) macrophages decreased in the aortic adventitia of $apoE^{-/-}$ mice with atherosclerosis ($P < 0.01$). Intimal lymphatics in the atherosclerotic lesions exhibited an atypical phenotype, with the expression of podoplanin and VEGF receptor 3 (VEGFR-3) but not of LYVE-1 and prospero homeobox protein 1. In the aortas of atherosclerotic animals, we found markedly increased soluble VEGFR-2. We hypothesized that the elevated soluble VEGFR-2 that was found in the aortas of $apoE^{-/-}$ mice with atherosclerosis binds to and diminishes the activity of VEGF-C. This trapping mechanism explains, despite increased VEGF-C in the atherosclerotic aortas, how adventitial lymphatics regress. Lymphatic regression impedes the drainage of lipids, growth factors, inflammatory cytokines, and immune cells. Insufficient lymphatic drainage could thus exacerbate atherosclerosis formation. Our study contributes new insights to previously unknown dynamic changes of adventitial lymphatics. Targeting soluble VEGFR-2 in atherosclerosis may provide a new strategy for the liberation of endogenous VEGF-C and the prevention of lymphatic regression.—Taher, M., Nakao, S., Zandi, S., Melhorn, M. I., Hayes, K. C., Hafezi-Moghadam, A. Phenotypic transformation of intimal and adventitial lymphatics in atherosclerosis: a regulatory role for soluble VEGF receptor 2. FASEB J. 30, 2490–2499 (2016). www.fasebj.org

KEY WORDS: lymphangiogenesis · LYVE-1 · podoplanin · macrophages · VEGF-C

INTRODUCTION

Atherosclerosis is a chronic inflammatory disease that involves both innate and adaptive immunity (1). As part of the inflammatory process, activated macrophages accumulate in the aortic wall and stimulate angiogenesis—the growth of new blood vessels—and thereby contribute to plaque formation (2). Angiogenesis in plaques is associated with plaque vulnerability (3). Accumulation of macrophages in atherosclerotic plaques represents an imbalance of macrophage recruitment from blood into the aortic wall and macrophage clearance from the plaques *via* lymphatics (4). In atherosclerosis, macrophage recruitment is increased as a result of angiogenesis and the presence of proinflammatory cytokines (5, 6). Lymphatics are expressed in human atherosclerosis (7, 8); however, little is known about the dynamics of lymphatic growth in the course of the formation of atherosclerosis.

Lymphatics are essential to immune function and key in such pathologies as cancer (9, 10). The role of lymphatics in atherosclerosis is just now undergoing study (11). The lymphatic endothelium heterogeneously expresses lymphatic vessel endothelial hyaluronan receptor 1 (LYVE-1), VEGF receptor 3 (VEGFR-3), podoplanin, and prospero homeobox protein 1

ABBREVIATIONS: $apoE^{-/-}$, apolipoprotein E–deficient; LYVE-1, lymphatic vessel endothelial hyaluronan receptor 1; M:F, male-to-female ratio; PROX1, prospero homeobox protein 1; VEGFR, VEGF receptor; WD, Western diet; WT, wild-type

[1] Correspondence: Brigham and Women's Hospital, 45 Francis St., Boston, MA 02115, USA. E-mail: ahm@bwh.harvard.edu

doi: 10.1096/fj.201500112
This article includes supplemental data. Please visit *http://www.fasebj.org* to obtain this information.

0892-6638/16/0030-2490 © FASEB

(PROX1) (9). Lymphangiogenesis, the growth of new lymphatics, shares several characteristics with angiogenesis, the growth of new blood vessels (12), and several factors that induce angiogenesis also promote lymphangiogenesis (13). These factors, members of the VEGF family and cytokines such as TNF-α, are elevated in chronic inflammatory conditions (14). Lymphangiogenesis and angiogenesis often accompany each other in chronic inflammatory conditions (15). Despite their commonalities and joined occurrence in pathologies, lymphangiogenesis and angiogenesis have distinct dissimilarities (12).

Lymphatic growth lags behind angiogenic growth (12). We found that actively growing blood vessels suppress lymphatic growth (12). The suppression occurs because the angiogenic endothelium competes for and binds with the growth factor that would otherwise induce the growth of the lymphatic endothelium (12). The endothelium of actively growing blood vessels expresses higher levels of VEGFR-2 (12). These endothelial VEGFR-2 molecules bind with and deplete the growth factor, VEGF-C, from the extracellular matrix (12). VEGFR-2 is proteolytically cleaved from the endothelial membrane (16). Similar to the membrane-bound form, soluble VEGFR-2 binds with VEGF-C and impedes its biologic activity.

VEGF-C has an affinity to endothelial VEGFR-2 but also to VEGFR-3 on the lymphatic endothelium. The binding of VEGF-C to VEGFR-3 induces lymphangiogenesis (14). The removal of VEGF-C by the angiogenic endothelium impedes lymphatic growth, whereas blood vessel endothelium thrives (12). This mechanism, which is termed receptor-mediated growth factor internalization, explains why lymphatics are not found together with actively growing blood vessels (12). Whether angiogenesis in atherosclerosis regulates lymphatic growth remains to be studied.

When angiogenic vessels mature, they downregulate their VEGFR-2 to the baseline levels that are found in normal quiescent endothelium (12). With VEGFR-2 expressed at low levels, the endothelium of the matured blood vessel no longer depletes extracellular VEGF-C. Consequently, VEGF-C signals *via* the lymphatic endothelial VEGFR-3 and induces lymphatic growth. This explains the temporal lag of lymphangiogenesis relative to angiogenesis, presumably until the newly formed blood vessels mature (12).

Apolipoprotein E–deficient ($apoE^{-/-}$) mice spontaneously develop atherosclerosis, and feeding them a Western diet (WD) further accelerates the process (17). Angiogenesis has been established in the context of atherosclerosis in these mice (18); however, lymphatics in the atherosclerotic lesions of these mice have not been studied. To explore lymphangiogenesis in the dynamic context of atherosclerosis formation, we examined aortas of young and aged $apoE^{-/-}$ mice. We further studied the burden of WD on their lymphatics in the aorta. In the aortas of these mice, we quantified immune cells, lymphatic markers, and soluble VEGFR-2.

TABLE 1. *Composition of the semipurified WD*

WD composition	
Ingredient	Amount
CHO/fat/protein (% calories)	60:20:20
Cholesterol (g/kg)	10
Casein (g/kg)	105
Lactalbumin (g/kg)	105
Dextrose (g/kg)	186
Sucrose (g/kg)	186
Cornstarch (g/kg)	194
Margarine B (80% fat) (g/kg)	116 (93 fat)
Mineral mix (g/kg)	46
Vitamin mix (g/kg)	12
Choline chloride (g/kg)	3

Carbohydrate, fat, and protein ratio (60:20:20% calories) represents the percentage of dietary calories provided by each nutrient category. Diet cholesterol was added at 1% by weight, and margarine B was a blend of fats common in the U.S. diet. It was based on saturated animal fat as 24% milk fat and 40% beef tallow, with sources of monounsaturated and polyunsaturated fats from 20% chicken fat and 16% soybean oil. The ratio of saturated to monounsaturated to polyunsaturated fatty acids was approximately 44:38:18. The diet was adjusted for vitamin and mineral concentrations as a percentage of calories (4.2 kcal/g). CHO, carbohydrate; prot, protein.

MATERIALS AND METHODS

Animals

Young (8- to 12-wk-old mice) and aged (54- to 58-wk-old retired breeders) C57BL/6J mice (000664; The Jackson Laboratory, Bar Harbor, ME, USA) and young (8- to 12-wk-old mice) and aged $apoE^{-/-}$ mice (54- to 58-wk-old retired breeders from our own colony) were housed in a temperature-controlled animal facility with a 12-h light/dark cycle and were fed standard laboratory chow and water ad libitum. To accelerate atherosclerosis formation, $apoE^{-/-}$ animals, starting at 6 wk of age, were fed a WD for 26 wk. For all experiments, we used both male and female mice and indicated the male-to-female ratio (M:F) for each experiment. All animal experiments were approved by the Institutional Animal Care and Use Committee of Brigham and Women's Hospital.

Diet

WD was made from semipurified components. The carbohydrate/fat/protein ratio was calculated as percentages of total calories and adjusted for vitamins and minerals (Table 1). The regular diet was in accordance to the standard composition, Formulab Diet 5008C33.

Plasma cholesterol and triglyceride measurements

Mouse blood (1 ml) was obtained through cardiac puncture under anesthesia. Heparinized blood was centrifuged at 12,500 rpm for 10 min at 4°C, and plasma was collected. Plasma total cholesterol levels and triglycerides were measured by using Thermo Infinity kits (Thermo Electron, Pittsburgh, PA, USA) and a serum triglyceride determination kit (Sigma-Aldrich, St. Louis, MO, USA), respectively.

Immunohistochemistry

Aortic trees were perfused with PBS, and aortic arches were harvested and snap-frozen in optimal cutting temperature

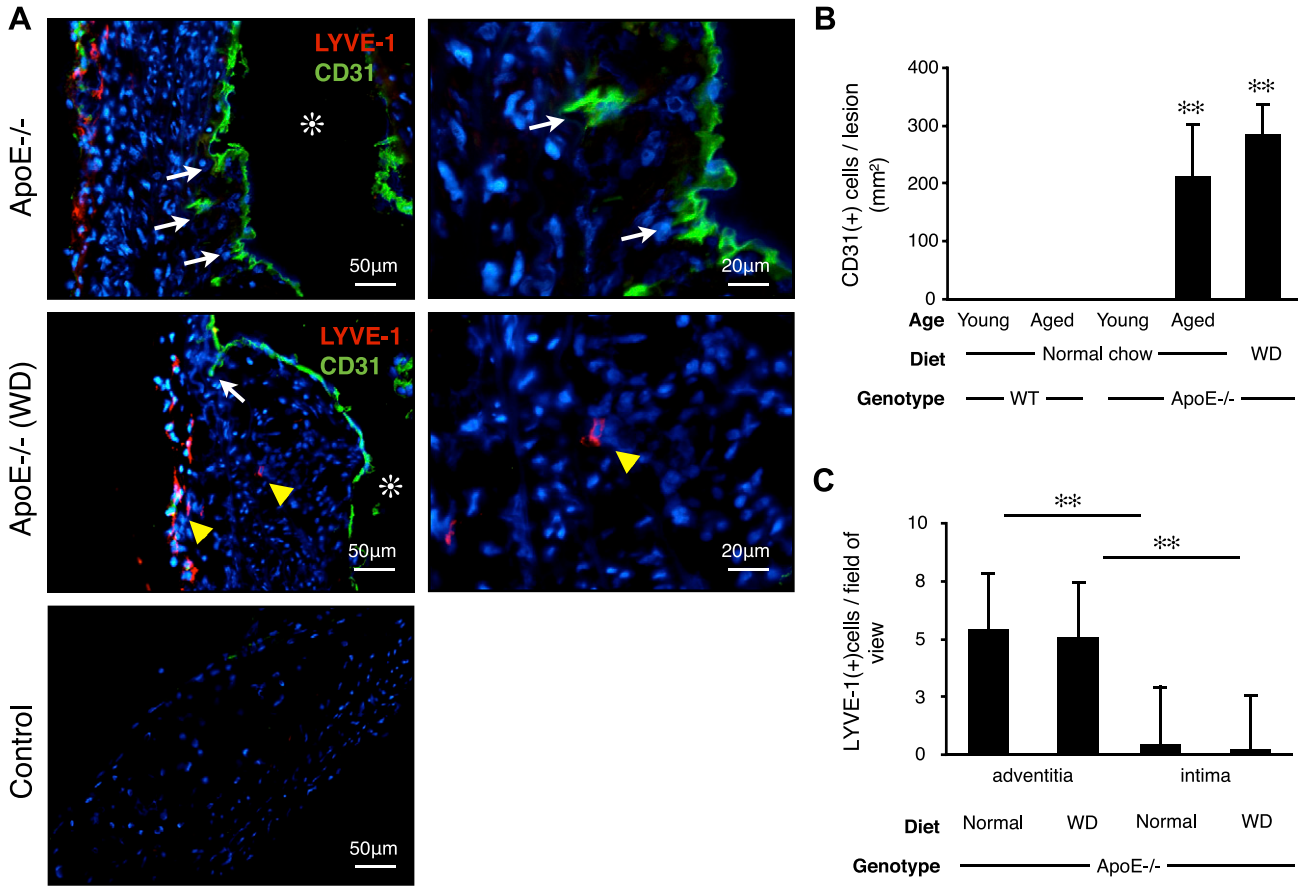

Figure 1. Scarcity of LYVE-1$^+$ cells in atherosclerotic plaques despite abundant angiogenesis. Vascular endothelium staining (CD31, green) and lymphatic endothelium staining (LYVE-1, *red*) in atherosclerotic lesions of *apoE*$^{-/-}$ mice. *A*) In aged *apoE*$^{-/-}$ mice fed normal diet ($n = 3$; 54–56 wk; M:F, 0.6) and in WD-fed *apoE*$^{-/-}$ mice ($n = 3$; 32 wk; M:F, 0.4), CD31$^+$ cells were found in the intimal space, which indicated angiogenesis (white arrows). Asterisks indicate aortic lumen; yellow arrowheads indicate LYVE-1$^+$ macrophages. *B*) Quantification of CD31$^+$ cells in the intima (aged *apoE*$^{-/-}$: $n = 3$; 54–56 wk; M:F, 0.6; WD: $n = 3$; 32 wk; M:F, 0.4), means ± SEM. *C*) Quantification of intimal *vs.* adventitial LYVE-1$^+$ cells (aged *apoE*$^{-/-}$: $n = 5$; 54–58 wk; M:F, 0.6; WD: $n = 3$; 32 wk; M:F, 0.4), means ± SEM. $^{**}P < 0.01$.

compound (Sakura Finetek, Torrance, CA, USA). Sections (10 μm) were prepared, air dried, and fixed in ice-cold acetone for 10 min. Sections were blocked with 3% nonfat dried milk bovine working solution (Sigma-Aldrich) and stained with anti-mouse CD31 mAb (1:50, 0.31 μg/ml; BD Pharmingen, Brea, CA, USA) and anti-mouse LYVE-1 Ab (1 μg/ml; ReliaTech, Wolfenbüttel, Germany), anti-mouse VEGFR-2 (5 μg/ml; R&D Systems, Minneapolis, MN, USA), or anti-mouse podoplanin (1 μg/ml; ReliaTech), anti-mouse VEGFR-3 (5 μg/ml; R&D Systems), anti-human PROX1 (5 μg/ml; R&D Systems), and CD11b (1:200, 0.63 μg/ml; BD Pharmingen). After an overnight incubation at 4°C, sections were washed and stained for 60 min at room temperature with Alexa Fluor 647 goat anti-rabbit IgG (2 μg/ml; Thermo Fisher Scientific Life Sciences, Waltham, MA, USA), Alexa Fluor 546 goat anti-rabbit IgG (2 μg/ml; Thermo Fisher Scientific Life Sciences), Alexa Fluor 488 goat anti-rat IgG (2 μg/ml; Thermo Fisher Scientific Life Sciences), and Alexa Fluor 488 goat anti-hamster IgG (2 μg/ml; Thermo Fisher Scientific Life Sciences).

Whole-mount immunofluorescence

Abdominal aortas were excised and fixed in 4% paraformaldehyde for 1 h at 4°C, washed in PBS and methanol, blocked in 10% goat serum and 1% Triton X-100, and stained with anti-mouse LYVE-1 Ab (4 μg/ml; ReliaTech) and anti-mouse CD31 mAb (1:12.5; BD Pharmingen) overnight at 4°C. Samples were washed and stained with Alexa Fluor 647 goat anti-rabbit IgG (20 μg/ml; Thermo Fisher Scientific Life Sciences) and Alexa Fluor 488 goat anti-rat IgG (20 μg/ml; Thermo Fisher Scientific Life Sciences) overnight at 4°C. Photomicrographs were obtained across the length of the entire aortic whole mount. Single images were subsequently merged with a mosaic whole mount by using ImageJ software with the MosaicJ plugin (National Institutes of Health, Bethesda, MD, USA). Lymphatic vasculature was measured as the sum of areas > 100-pixel threshold and expressed as the ratio of lymphatics to the entire area of the whole mount.

Western blot

Aortic trees were perfused *in situ* with PBS. Whole aortas were harvested, minced, and snap-frozen. Of RIPA lysis buffer (Sigma-Aldrich), 200 μl was added to each minced aorta. RIPA lysis buffer was prepared to contain protease and phosphatase inhibitors (P2850, P5726, P8340; Sigma-Aldrich). Tissues were homogenized with a tissue homogenizer and centrifuged (12,500 rpm for 10 min at 4°C). Supernatants were collected, and protein concentrations were measure by using protein assay (Bio-Rad, Hercules, CA, USA). Equal amounts of total protein were loaded onto SDS-PAG (Bio-Rad). Gels were run at 170 V for ~40 min.

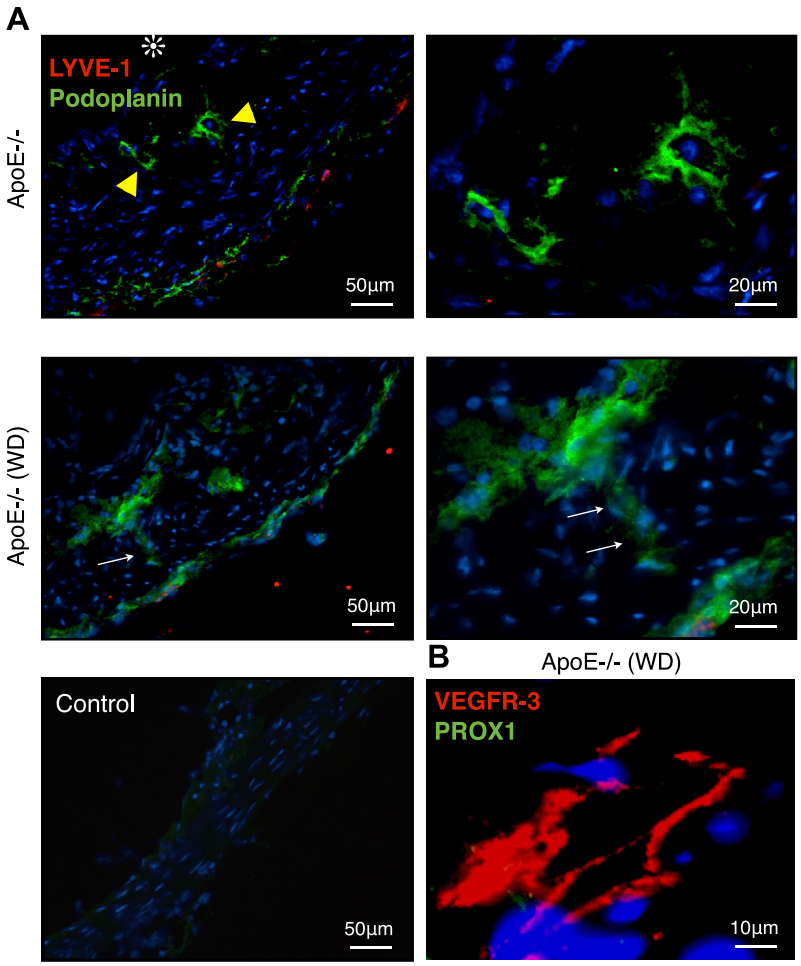

Figure 2. Podoplanin$^+$ LYVE-1$^-$ tube-like structures in atherosclerotic lesions. Double immunofluorescence staining for lymphatic endothelial markers, LYVE-1 (red) and podoplanin (green) in atherosclerotic lesions of *apoE*$^{-/-}$ mice. *A*) In aged *apoE*$^{-/-}$ mice fed normal diet ($n = 5$; 54–58 wk; M:F, 0.6) and in WD-fed *apoE*$^{-/-}$ mice ($n = 3$; 32 wk; M:F, 0.4), podoplanin$^+$ LYVE-1$^-$ tube-like structures were found in the intimal space (yellow arrowheads). Podoplanin$^+$ LYVE-1$^-$ tube-like structure crossing the intimal media border (white arrows). *B*) Immunofluorescence staining for the lymphatic endothelial markers, VEGFR-3 (red) and PROX1 (green). Intimal lymphatic-like structures expressed VEGFR-3 but not PROX1.

Proteins were transferred from gels to Immobilon PVDF membranes (Millipore, Bedford, MA, USA). Blots were blocked with 5% nonfat dry milk, washed, then incubated with anti-mouse VEGFR-2 (0.2 μg/ml; R&D Systems; or 1:1000; Cell Signaling Technologies, Danvers, MA, USA), anti-mouse LYVE-1 (4 μg/ml; ReliaTech), anti-mouse podoplanin (1 μg/ml; ReliaTech), anti-human VEGF-C (1 μg/ml; R&D Systems), and anti-mouse ERK-2 (0.5 μg/ml; Santa Cruz Biotechnology, Dallas, TX, USA) antibodies overnight at 4°C. Blots were washed and incubated with secondary Abs coupled to horseradish peroxidase for 1 h at room temperature, and protein bands were visualized by using ECL technology (GE Healthcare Life Sciences, Pittsburgh, PA, USA).

Statistical analysis

All results are expressed as mean ± SEM, and n numbers are as indicated. For statistical comparison between 2 groups, we used 2-tailed Student's t test, and ANOVA was used for comparison between multiple groups. A χ^2 test was used to examine the odds ratios of expressions of podoplanin$^+$ lymphatic-like structures in the atherosclerotic lesions. Differences between means were considered statistically significant at $P < 0.05$.

RESULTS

Scarce LYVE-1$^+$ cells in atherosclerotic lesions

To investigate lymphangiogenesis in the context of atherosclerosis, we stained aortic arches from wild-type (WT) and *apoE*$^{-/-}$ mice for the endothelial marker CD31 and the lymphatic endothelial marker LYVE-1. WT animals, young and aged, did not develop atherosclerosis, and CD31 staining was restricted to the luminal endothelial layer (data not shown). Aged and WD-fed *apoE*$^{-/-}$ mice developed atherosclerotic lesions and angiogenesis, which was evidenced by interstitial proliferation and CD31$^+$ staining in the aortic intima (**Fig. 1*A***). The atherosclerotic lesions of aged *apoE*$^{-/-}$ mice that were fed normal chow and *apoE*$^{-/-}$ mice fed WD showed comparable levels of CD31$^+$ cells (Fig. 1*B*). Only 22 LYVE-1$^+$ single cells were counted in 48 examined atherosclerotic lesions of WD-fed *apoE*$^{-/-}$ mice and 54 LYVE-1$^+$ single cells in 102 examined atherosclerotic lesions of aged *apoE*$^{-/-}$ mice fed normal diet. These data show that LYVE-1$^+$ single cells are rather rare in atherosclerotic lesions. This is unusual because angiogenesis and lymphangiogenesis are commonly accompanied by LYVE-1$^+$ macrophages.

To account for the potential role of plasma lipids, we measured total cholesterol and triglycerides in our experimental animals. Total cholesterol levels were significantly higher in *apoE*$^{-/-}$ mice compared with WT mice. Total cholesterol levels increased with age in *apoE*$^{-/-}$ mice but not in WT animals (Supplemental Fig. 1).

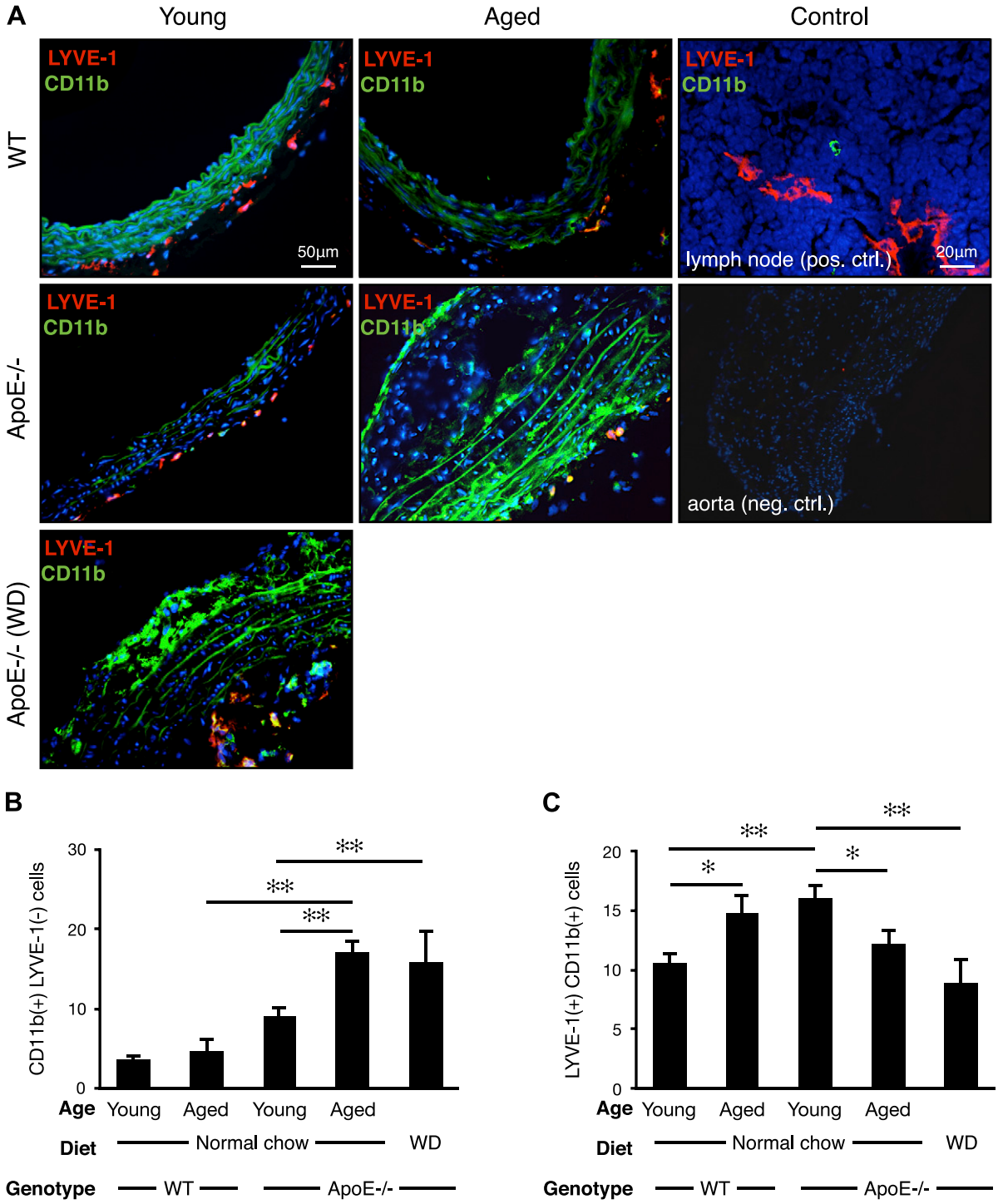

Figure 3. Age dependence of adventitial LYVE-1$^+$ cells. Immunofluorescence staining for lymphatic endothelium (LYVE-1, red) and the leukocyte activation marker, CD11b (green). *A*) Aortic arch cryosections. Lymph node, positive control. *B, C*) Quantification of adventitial CD11b$^+$ LYVE-1$^-$ cells (*B*) and LYVE-1$^+$ CD11b$^+$ cells (*C*) (young WT mice: $n = 5$; 8–12 wk; M:F, 0.6; aged WT mice: $n = 5$; 54–58 wk; M:F, 0.6; young *apoE*$^{-/-}$ mice: $n = 5$; 8–12 wk; M:F, 0.6; aged *apoE*$^{-/-}$ mice: $n = 5$; 54–58 wk; M:F, 0.6; WD: $n = 3$; 32 wk; M:F, 0.6), means ± SEM. $^*P < 0.05$, $^{**}P < 0.01$.

Unique LYVE-1$^-$ lymphatic-like structures in atherosclerotic lesions

To investigate lymphatic expression in atherosclerotic lesions, we stained for podoplanin, an established marker for lymphatic endothelium, in the aortas of *apoE*$^{-/-}$ mice. Atherosclerotic lesions showed podoplanin$^+$ tube-like structures, which did not coimmunostain with LYVE-1 (**Fig. 2*A***). Some of the podoplanin$^+$ lymphatics breached the intima-media border and built a vascular connection between these two layers (Fig. 2*A*, arrows). To confirm

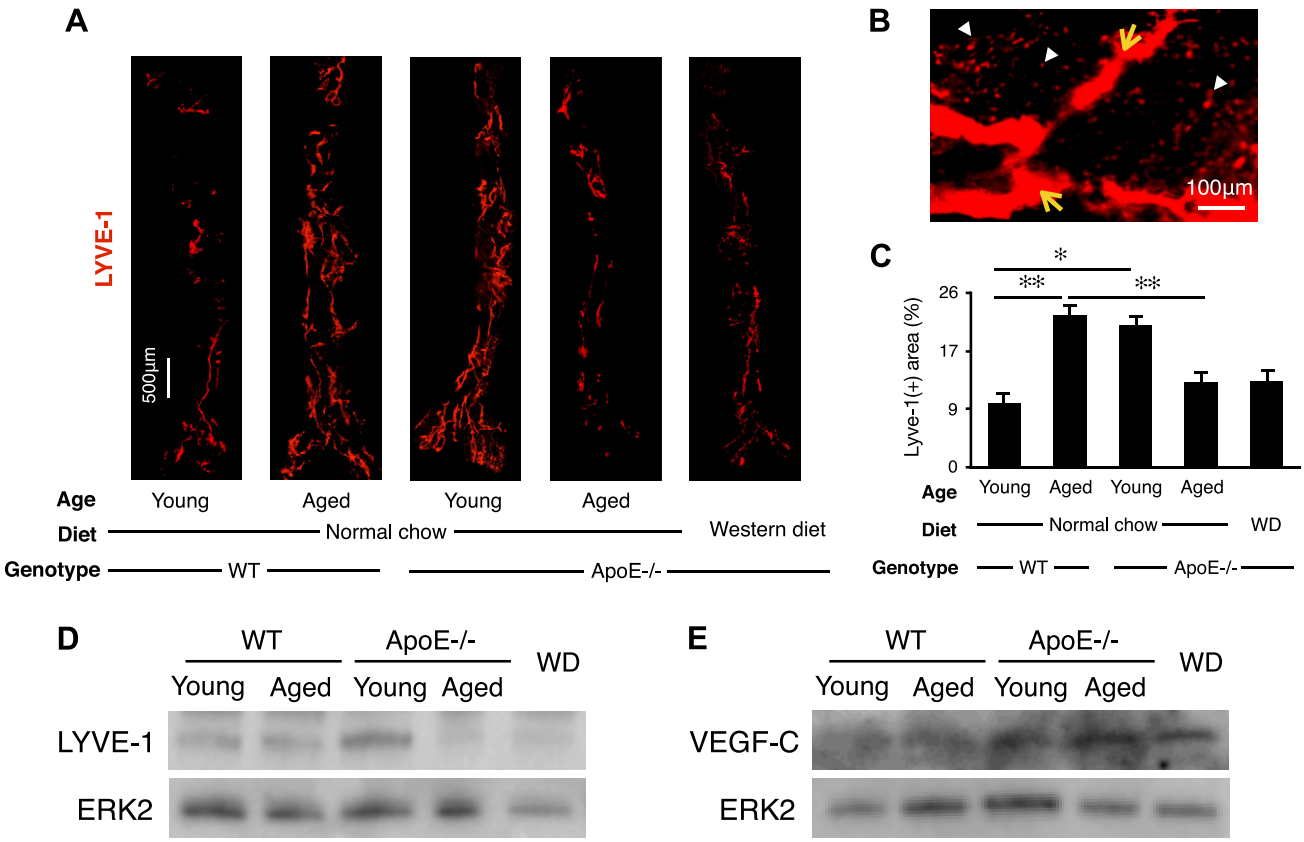

Figure 4. Adventitial lymphangiogenesis. *A*) Whole-mount immunofluorescence staining for LYVE-1$^+$ lymphatic vascular structures (red). Adventitial vessels are visualized in abdominal aortas (young WT mice: $n = 5$; 8–12 wk; M:F, 0.6; aged WT mice: $n = 5$; 54–58 wk; M:F, 0.6; young *apoE*$^{-/-}$ mice: $n = 5$; 8–12 wk; M:F, 0.6; aged *apoE*$^{-/-}$ mice: $n = 5$; 54–58 wk; M:F, 0.6; WD: $n = 4$; 32 wk; M:F, 0.5). Micrographs represent mosaics that were created by merging adjacent photomicrographs by using ImageJ. *B*) Photomicrograph of a representative atherosclerotic aorta illustrating LYVE-1$^+$ lymphatic capillaries surrounded by LYVE-1$^+$ macrophages (32-wk-old male, WD-fed *apoE*$^{-/-}$ mouse). *C*) Quantification of the LYVE-1$^+$ areas as a percentage of the total aortic flatmount areas (young WT mice: $n = 5$; 8–12 wk; M:F, 0.6; aged WT mice: $n = 5$; 54–58 wk; M:F, 0.6; young *apoE*$^{-/-}$ mice: $n = 5$; 8–12 wk; M:F, 0.6; aged *apoE*$^{-/-}$ mice: $n = 5$; 54–58 wk; M:F, 0.6; WD: $n = 4$; 32 wk; M:F, 0.5). *D*) Western blot analysis of LYVE-1 in aortic walls, ERK-2 loading control (young WT mice: $n = 4$; 8–12 wk; M:F, 0.5; aged WT mice: $n = 4$; 54–58 wk; M:F, 0.5; young *apoE*$^{-/-}$ mice: $n = 4$; 8–12 wk; M:F, 0.5; aged *apoE*$^{-/-}$ mice: $n = 4$; 54–58 wk; M:F, 0.5; WD: $n = 4$; 32 wk; M:F, 0.5). *E*) Western blot analysis of VEGF-C in aortic walls, ERK-2 loading control (young WT mice: $n = 4$; 8–12 wk; M:F, 0.5; aged WT mice: $n = 4$; 54–58 wk; M:F, 0.5; young *apoE*$^{-/-}$ mice: $n = 4$; 8–12 wk; M:F, 0.5; aged *apoE*$^{-/-}$ mice: $n = 4$; 54–58 wk; M:F, 0.5; WD: $n = 4$; 32 wk; M:F, 0.5). *F*) Aortic arch cryosections. *G*) Quantification of adventitial podoplanin$^+$ LYVE-1$^-$ cells (young WT mice: $n = 5$; 8–12 wk; M:F, 0.6; aged WT mice: $n = 5$; 54–58 wk; M:F, 0.6; young *apoE*$^{-/-}$ mice: $n = 5$; 8–12 wk; M:F, 0.6; aged *apoE*$^{-/-}$ mice: $n = 5$; 54–58 wk; M:F, 0.6; WD: $n = 3$; 32 wk; M:F, 0.6), means ± SEM. $^*P < 0.05$, $^{**}P < 0.01$.

that these podoplanin$^+$ tube-like structures are of lymphatic origin, we stained for VEGFR-3 and found specific staining. Unexpectedly, these vessels did not stain for the lymphatic endothelial marker, PROX1 (Fig. 2*B*).

In aged *apoE*$^{-/-}$ mice fed normal diet, 33% (8 of 24) of the examined atherosclerotic lesions showed podoplanin$^+$ lymphatics in the intima, whereas in WD-fed *apoE*$^{-/-}$ mice, 83% (15 of 18) of the examined lesions showed such lymphatics ($P < 0.01$; aged *apoE*$^{-/-}$: $n = 5$; 54–58 wk; M:F, 0.6; WD: $n = 3$; 32 wk; M:F, 0.4).

Reduced LYVE-1$^+$ cells in atherosclerosis

To examine adventitial inflammation as a source of prolymphangiogenic factors, we stained aortic sections with the leukocyte activation marker, CD11b, as well as with the lymphatic endothelial marker, LYVE-1 (19). Both CD11b$^+$ and LYVE-1$^+$ cells were found in the aortic adventitia of young and aged WT and *apoE*$^{-/-}$ mice as well as in the young WD-fed *apoE*$^{-/-}$ mice (**Fig. 3*A***).

The number of activated CD11b$^+$/LYVE-1$^-$ leukocytes remained unchanged in aged WT mice compared with young WT mice; however, the numbers of these cells were significantly higher in aged *apoE*$^{-/-}$ mice and in and WD-diet fed *apoE*$^{-/-}$ mice (Fig. 3*B*). This is in line with the notion that diet burden and age may increase inflammation.

Unexpectedly, the number of LYVE-1$^+$/CD11b$^+$ cells significantly decreased with disease progression, that is, in aged *apoE*$^{-/-}$ mice and in WD-fed *apoE*$^{-/-}$ mice (Fig. 3*C*). In WT mice, the number of these cells increased with

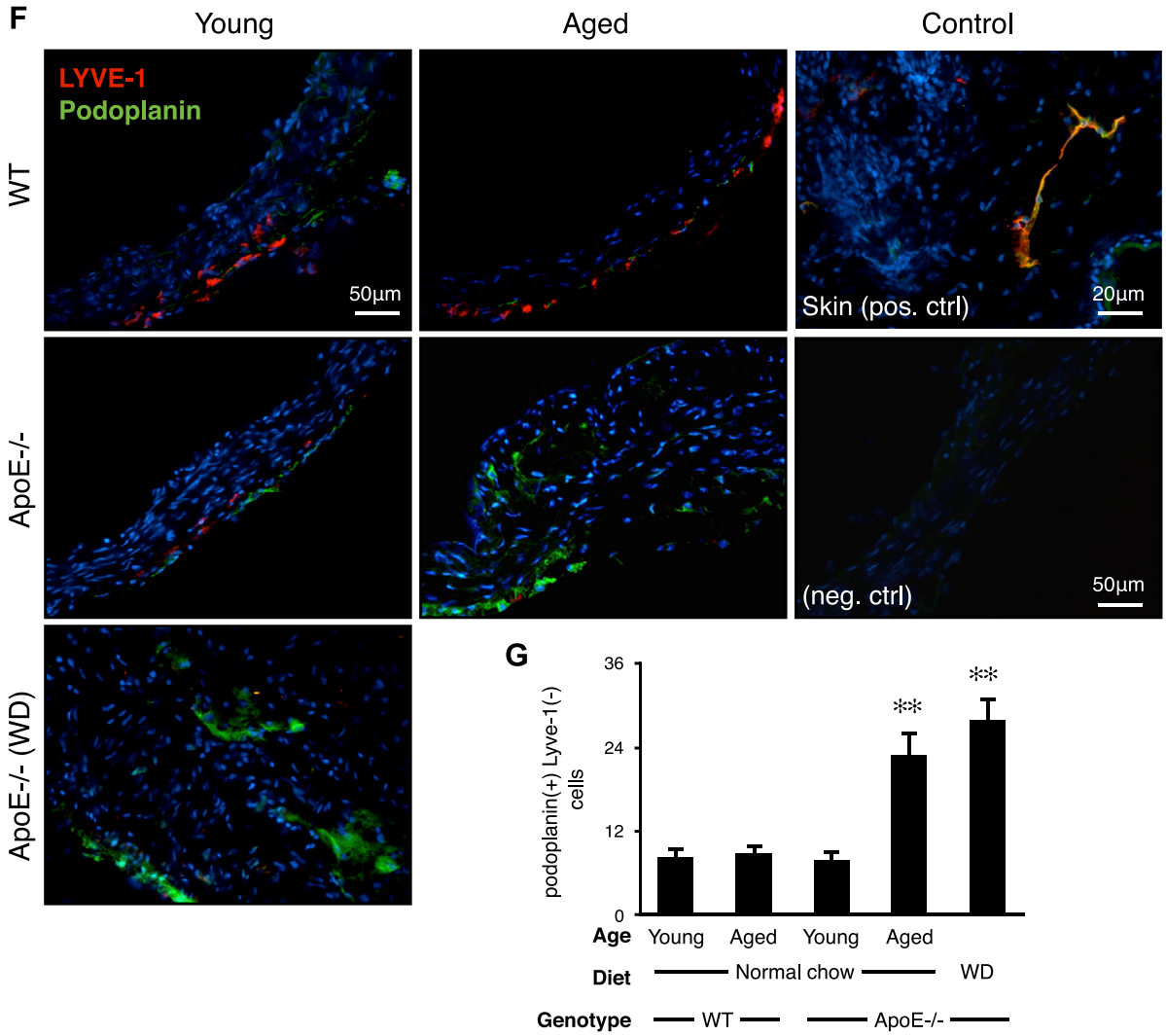

Figure 4. (*continued*)

age. Young *apoE*$^{-/-}$ mice fed normal diet had higher levels of LYVE-1^{+}/CD11b^{+} cells compared with young WT mice (Fig. 3*C*).

Unexpected reduction in LYVE-1^{+} but not podoplanin^{+} adventitial lymphatics in atherosclerosis

To quantify adventitial lymphatics, we performed whole-mount staining of abdominal aortas for LYVE-1 (**Fig. 4*A***). Whole mounts showed LYVE-1^{+} tube-like structures in the adventitia. Whole-mount staining showed that LYVE-1^{+} lymphatics were surrounded by LYVE-1^{+} macrophages, which were distinguished by their characteristic morphologies (Fig. 4*B*).

In WT mice, LYVE-1^{+} adventitial lymphatic vessels increased with age (Fig. 4*C*). Young *apoE*$^{-/-}$ mice showed significantly more LYVE-1^{+} adventitial lymphatics than did age-matched WT mice. Unexpectedly, the amount of adventitial lymphatics in aged *apoE*$^{-/-}$ mice was significantly less than that in young *apoE*$^{-/-}$ mice (Fig. 4*C*). In contrast to their reduced amounts of adventitial lymphatics, aged *apoE*$^{-/-}$, but not aged WT mice, showed significant amounts of adventitial angiogenic vessels (Supplemental Fig. 2). WD-fed *apoE*$^{-/-}$ mice showed a low level of adventitial lymphatics similar to that of aged *apoE*$^{-/-}$ mice fed normal chow (Fig. 4*C*), which suggested a role for plasma lipids in the regression of adventitial lymphatics.

We performed Western blot analysis for LYVE-1 in aortas from the various groups. Results confirmed a reduction of LYVE-1 in aged *apoE*$^{-/-}$ mice and in WD-fed *apoE*$^{-/-}$ mice (Fig. 4*D*).

To investigate a potential cause of LYVE-1 reduction, we performed Western blot analysis for the lymphangiogenic growth factor, VEGF-C, in the aortas from the various groups. Unlike LYVE-1, VEGF-C did not decline in aged *apoE*$^{-/-}$ fed normal diet or in WD-fed *apoE*$^{-/-}$ mice (Fig. 4*E*).

As an important marker of lymphatics, we examined podoplanin expression in the adventitia (Fig. 4*F*). In contrast to LYVE-1, the number of podoplanin^{+} cells increased in aged *apoE*$^{-/-}$ mice and in WD-fed *apoE*$^{-/-}$ mice (Fig. 4*G*).

Elevated soluble VEGFR-2 expression in atherosclerotic aortas

We next investigated the expression of VEGFR-2 in immunohistochemistry. In all examined aortas, VEGFR-2 colocalized with luminal CD31$^+$ endothelial cells (**Fig. 5*A***). In atherosclerotic lesions in *apoE*$^{-/-}$ mice, VEGFR-2 was expressed in the intimal angiogenic vessels that costained for CD31 (Fig. 5*A*).

To explore potential mechanisms for the adventitial LYVE-1 regression, and despite the elevated VEGF-C in atherosclerotic aortas, we quantified the expression of soluble VEGFR-2 in the aortas. We performed Western blot analysis for soluble VEGFR-2. The expression of the 75 kDA soluble VEGFR-2 splice variant was significantly higher in aged *apoE*$^{-/-}$ mice fed regular diet as well as in WD-fed *apoE*$^{-/-}$ mice compared with controls.

DISCUSSION

In atherosclerosis, intimal and adventitial angiogenesis are correlated with disease progression (2, 20); however, the expression and function of lymphatics in atherosclerosis are less well understood (21). We discovered a surprising regression of adventitial lymphatics and a reduction in LYVE-1$^+$ macrophages with atherosclerosis. LYVE-1$^+$ macrophages are key contributors to lymphangiogenesis (19). In contrast to the adventitia, in which these cells abound, few LYVE-1$^+$ cells were found in the intima.

A lack of classic lymphatics, in which angiogenic vessels proliferate, is intriguing as lymphangiogenesis and angiogenesis are closely related processes that are often caused by the same factors (9). Yet, despite the prolymphangiogenic milieu of the atherosclerotic aortas, which is evidenced by increased VEGF-C, there is a paucity of classic lymphangiogenesis in the atherosclerotic lesions and even lymphatic regression in the adventitia.

To investigate the mechanism that underlies the adventitial lymphatic regression, we considered whether VEGF-C is potentially trapped by VEGFR-2, as we previously showed (12). Angiogenic endothelial cells express higher levels of VEGFR-2. We showed angiogenesis and VEGFR-2 expression in atherosclerotic aortas both in the intimal and adventitia,

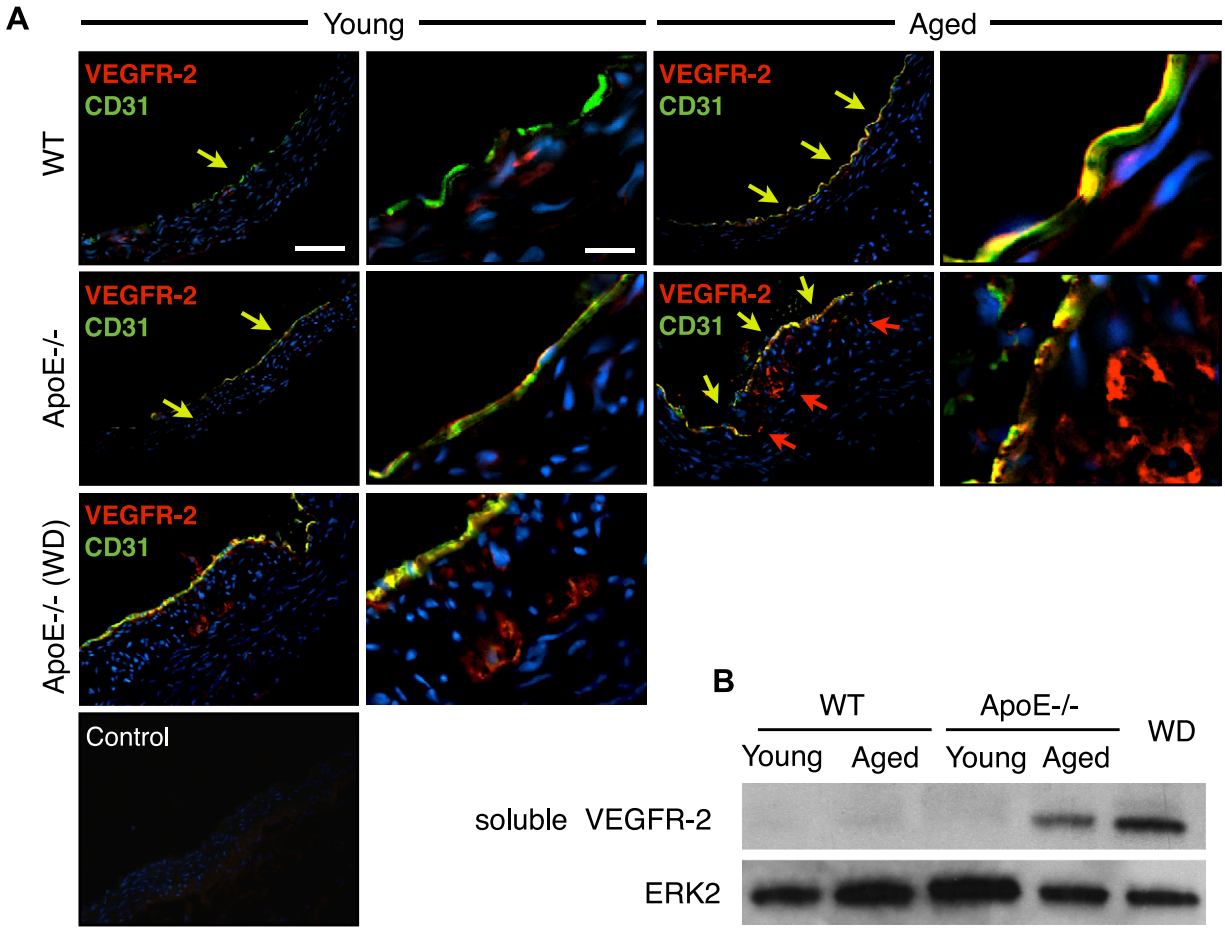

Figure 5. VEGFR-2 and soluble VEGFR-2 in aortas of aged and atherosclerotic mice. *A*) Immunofluorescence staining for VEGFR-2 (red) and the vascular endothelial cell marker, CD31 (green). Coimmunostaining for CD31 and VEGFR-2 (yellow arrows) and VEGFR-2 staining (red arrows). *B*) Western blot analysis for soluble VEGFR-2 (75 kDa) protein in aortic walls, ERK-2 loading control (young WT mice: $n = 4$; 8–12 wk; M:F, 0.5; aged WT mice: $n = 4$; 54–58 wk; M:F, 0.5; young *apoE*$^{-/-}$ mice: $n = 4$; 8–12 wk; M:F, 0.5; aged *apoE*$^{-/-}$ mice: $n = 4$; 54–58 wk; M:F, 0.5; WD: $n = 4$; 32 wk; M:F, 0.5).

and we found elevated levels of soluble VEGFR-2 in atherosclerosis. VEGF-C molecules, trapped by VEGFR-2, no longer promote growth of lymphatic endothelium (12). Other factors, including plasma lipids and inflammatory cytokines, may also contribute to the regression of adventitial lymphatics in atherosclerosis.

We found atypical lymphatic-like tubes in the intima in atherosclerotic lesions in mice. In contrast to classic lymphatic capillaries, the intimal lymphatic-like capillaries expressed 2 lymphatic markers, podoplanin and VEGFR-3, but did not express 2 other lymphatic markers, LYVE-1 and PROX1. To our knowledge, this is the first description of atypical lymphatic-like structures in atherosclerotic lesions. LYVE-1 is down-regulated by TNF-α (22), and TNF-α is elevated in atherosclerotic lesions (23, 24) and in plasma during atherosclerosis (25). The lack of LYVE-1 in the intimal lymphatic-like capillaries, thus, could be associated with elevated TNF-α found in atherosclerosis (23, 24).

Furthermore, we found elevated podoplanin expression in the intima and adventitia during atherosclerosis. Podoplanin stimulates platelet aggregation (26). The elevated podoplanin in the lymphatic-like capillaries could thus enhance the thrombogenicity of atherosclerotic plaques.

Our results show a correlation between atherosclerosis formation, increased soluble VEGFR-2 expression, and adventitial lymphatic regression. To our knowledge, this correlation is novel and introduces a new parameter to the pathogenesis. Adventitial lymphatics absorb interstitial fluids through the aortic wall, which is essential for normal tissue maintenance (27, 28). Lymphatic regression could impede the drainage of lipids, growth factors, inflammatory cytokines, and immune cells. Our hypothesis that lymphatic regression could drive atherosclerosis contrasts with the established paradigm that the inhibition of lymphangiogenesis could halt atherosclerosis (29). A beneficial effect of monocyte-derived migration from atherosclerotic plaques *via* lymphatics has been shown (4). Furthermore, the therapeutic effects of VEGF-C during myocardial infarction have recently been demonstrated (30). Our finding that soluble VEGFR-2 is elevated in atherosclerosis and might underlie the adventitial lymphatic regression *via* trapping of VEGF-C opens new possibilities for therapeutic targeting. FJ

The authors thank the Malaysian Palm Oil Board. This work was supported by a DP3 IMPACT award from U.S. National Institutes of Health, National Institute of Diabetes and Digestive and Kidney Diseases Grant DK108238; a DiaComp award (to A.H.-M.); an overseas doctoral fellowship from the German Academic Exchange Service-DAAD (to M.T.); an overseas Research Fellowship Award from Bausch & Lomb; a fellowship award from the Japan Eye Bank Association; and a Tear Film and Ocular Surface Society Young Investigator Fellowship (to S.N.).

REFERENCES

1. Hansson, G. K., and Libby, P. (2006) The immune response in atherosclerosis: a double-edged sword. *Nat. Rev. Immunol.* **6**, 508–519
2. Moulton, K. S., Vakili, K., Zurakowski, D., Soliman, M., Butterfield, C., Sylvin, E., Lo, K.-M., Gillies, S., Javaherian, K., and Folkman, J. (2003) Inhibition of plaque neovascularization reduces macrophage accumulation and progression of advanced atherosclerosis. *Proc. Natl. Acad. Sci. USA* **100**, 4736–4741
3. Virmani, R., Kolodgie, F. D., Burke, A. P., Finn, A. V., Gold, H. K., Tulenko, T. N., Wrenn, S. P., and Narula, J. (2005) Atherosclerotic plaque progression and vulnerability to rupture: angiogenesis as a source of intraplaque hemorrhage. *Arterioscler. Thromb. Vasc. Biol.* **25**, 2054–2061
4. Llodrá, J., Angeli, V., Liu, J., Trogan, E., Fisher, E. A., and Randolph, G. J. (2004) Emigration of monocyte-derived cells from atherosclerotic lesions characterizes regressive, but not progressive, plaques. *Proc. Natl. Acad. Sci. USA* **101**, 11779–11784
5. Tanaka, K., Nagata, D., Hirata, Y., Tabata, Y., Nagai, R., and Sata, M. (2011) Augmented angiogenesis in adventitia promotes growth of atherosclerotic plaque in apolipoprotein E-deficient mice. *Atherosclerosis* **215**, 366–373
6. Drechsler, M., Duchene, J., and Soehnlein, O. (2015) Chemokines control mobilization, recruitment, and fate of monocytes in atherosclerosis. *Arterioscler. Thromb. Vasc. Biol.* **35**, 1050–1055
7. Nakano, T., Nakashima, Y., Yonemitsu, Y., Sumiyoshi, S., Chen, Y. X., Akishima, Y., Ishii, T., Iida, M., and Sueishi, K. (2005) Angiogenesis and lymphangiogenesis and expression of lymphangiogenic factors in the atherosclerotic intima of human coronary arteries. *Hum. Pathol.* **36**, 330–340
8. Grzegorek, I., Drozdz, K., Chmielewska, M., Gomulkiewicz, A., Jablonska, K., Piotrowska, A., Karczewski, M., Janczak, D., Podhorska-Okolow, M., Dziegiel, P., and Szuba, A. (2014) Arterial wall lymphangiogenesis is increased in the human iliac atherosclerotic arteries: involvement of CCR7 receptor. *Lymphat. Res. Biol.* **12**, 222–231
9. Nakao, S., Zandi, S., Faez, S., Kohno, R., and Hafezi-Moghadam, A. (2012) Discontinuous LYVE-1 expression in corneal limbal lymphatics: dual function as microvalves and immunological hot spots. *FASEB J.* **26**, 808–817
10. Zheng, W., Aspelund, A., and Alitalo, K. (2014) Lymphangiogenic factors, mechanisms, and applications. *J. Clin. Invest.* **124**, 878–887
11. Aspelund, A., Robciuc, M. R., Karaman, S., Makinen, T., and Alitalo, K. (2016) Lymphatic System in Cardiovascular Medicine. *Circ. Res.* **118**, 515–530
12. Nakao, S., Zandi, S., Hata, Y., Kawahara, S., Arita, R., Schering, A., Sun, D., Melhorn, M. I., Ito, Y., Lara-Castillo, N., Ishibashi, T., and Hafezi-Moghadam, A. (2011) Blood vessel endothelial VEGFR-2 delays lymphangiogenesis: an endogenous trapping mechanism links lymph- and angiogenesis. *Blood* **117**, 1081–1090
13. Tammela, T., and Alitalo, K. (2010) Lymphangiogenesis: Molecular mechanisms and future promise. *Cell* **140**, 460–476
14. Lohela, M., Bry, M., Tammela, T., and Alitalo, K. (2009) VEGFs and receptors involved in angiogenesis versus lymphangiogenesis. *Curr. Opin. Cell Biol.* **21**, 154–165
15. Nakao, S., Noda, K., Zandi, S., Sun, D., Taher, M., Schering, A., Xie, F., Mashima, Y., and Hafezi-Moghadam, A. (2011) VAP-1-mediated M2 macrophage infiltration underlies IL-1β- but not VEGF-A-induced lymph- and angiogenesis. *Am. J. Pathol.* **178**, 1913–1921
16. Donners, M. M., Wolfs, I. M., Olieslagers, S., Mohammadi-Motahhari, Z., Tchaikovski, V., Heeneman, S., van Buul, J. D., Caolo, V., Molin, D. G., Post, M. J., and Waltenberger, J. (2010) A disintegrin and metalloprotease 10 is a novel mediator of vascular endothelial growth factor-induced endothelial cell function in angiogenesis and is associated with atherosclerosis. *Arterioscler. Thromb. Vasc. Biol.* **30**, 2188–2195
17. Plump, A. S., Smith, J. D., Hayek, T., Aalto-Setälä, K., Walsh, A., Verstuyft, J. G., Rubin, E. M., and Breslow, J. L. (1992) Severe hypercholesterolemia and atherosclerosis in apolipoprotein E-deficient mice created by homologous recombination in ES cells. *Cell* **71**, 343–353
18. Moulton, K. S., Heller, E., Konerding, M. A., Flynn, E., Palinski, W., and Folkman, J. (1999) Angiogenesis inhibitors endostatin or TNP-470 reduce intimal neovascularization and plaque growth in apolipoprotein E-deficient mice. *Circulation* **99**, 1726–1732
19. Maruyama, K., Ii, M., Cursiefen, C., Jackson, D. G., Keino, H., Tomita, M., Van Rooijen, N., Takenaka, H., D'Amore, P. A., Stein-Streilein, J., Losordo, D. W., and Streilein, J. W. (2005) Inflammation-induced lymphangiogenesis in the cornea arises from CD11b-positive macrophages. *J. Clin. Invest.* **115**, 2363–2372

20. Langheinrich, A. C., Michniewicz, A., Sedding, D. G., Walker, G., Beighley, P. E., Rau, W. S., Bohle, R. M., and Ritman, E. L. (2006) Correlation of vasa vasorum neovascularization and plaque progression in aortas of apolipoprotein E(-/-)/low-density lipoprotein(-/-) double knockout mice. *Arterioscler. Thromb. Vasc. Biol.* **26**, 347–352
21. Kutkut, I., Meens, M. J., McKee, T. A., Bochaton-Piallat, M. L., and Kwak, B. R. (2015) Lymphatic vessels: an emerging actor in atherosclerotic plaque development. *Eur. J. Clin. Invest.* **45**, 100–108
22. Johnson, L. A., Prevo, R., Clasper, S., and Jackson, D. G. (2007) Inflammation-induced uptake and degradation of the lymphatic endothelial hyaluronan receptor LYVE-1. *J. Biol. Chem.* **282**, 33671–33680
23. Missiou, A., Köstlin, N., Varo, N., Rudolf, P., Aichele, P., Ernst, S., Münkel, C., Walter, C., Stachon, P., Sommer, B., Pfeifer, D., Zirlik, K., MacFarlane, L., Wolf, D., Tsitsikov, E., Bode, C., Libby, P., and Zirlik, A. (2010) Tumor necrosis factor receptor-associated factor 1 (TRAF1) deficiency attenuates atherosclerosis in mice by impairing monocyte recruitment to the vessel wall. *Circulation* **121**, 2033–2044
24. Liu, Z., Lerman, L. O., Tang, H., Barber, C., Wan, L., Hui, M. M., Furenlid, L. R., and Woolfenden, J. M. (2014) Inflammation imaging of atherosclerosis in Apo-E-deficient mice using a (99m)Tc-labeled dual-domain cytokine ligand. *Nucl. Med. Biol.* **41**, 785–792
25. Du, F., Yu, F., Wang, Y., Hui, Y., Carnevale, K., Fu, M., Lu, H., and Fan, D. (2014) MicroRNA-155 deficiency results in decreased macrophage inflammation and attenuated atherogenesis in apolipoprotein E-deficient mice. *Arterioscler. Thromb. Vasc. Biol.* **34**, 759–767
26. Cueni, L. N., Chen, L., Zhang, H., Marino, D., Huggenberger, R., Alitalo, A., Bianchi, R., and Detmar, M. (2010) Podoplanin-Fc reduces lymphatic vessel formation in vitro and in vivo and causes disseminated intravascular coagulation when transgenically expressed in the skin. *Blood* **116**, 4376–4384
27. Veerman, K. J., Venegas-Pino, D. E., Shi, Y., Khan, M. I., Gerstein, H. C., and Werstuck, G. H. (2013) Hyperglycaemia is associated with impaired vasa vasorum neovascularization and accelerated atherosclerosis in apolipoprotein-E deficient mice. *Atherosclerosis* **227**, 250–258
28. Vuorio, T., Nurmi, H., Moulton, K., Kurkipuro, J., Robciuc, M. R., Ohman, M., Heinonen, S. E., Samaranayake, H., Heikura, T., Alitalo, K., and Ylä-Herttuala, S. (2014) Lymphatic vessel insufficiency in hypercholesterolemic mice alters lipoprotein levels and promotes atherogenesis. *Arterioscler. Thromb. Vasc. Biol.* **34**, 1162–1170
29. Kholová, I., Dragneva, G., Cermáková, P., Laidinen, S., Kaskenpää, N., Hazes, T., Cermáková, E., Steiner, I., and Ylä-Herttuala, S. (2011) Lymphatic vasculature is increased in heart valves, ischaemic and inflamed hearts and in cholesterol-rich and calcified atherosclerotic lesions. *Eur. J. Clin. Invest.* **41**, 487–497
30. Klotz, L., Norman, S., Vieira, J. M., Masters, M., Rohling, M., Dubé, K. N., Bollini, S., Matsuzaki, F., Carr, C. A., and Riley, P. R. (2015) Cardiac lymphatics are heterogeneous in origin and respond to injury. *Nature* **522**, 62–67

Received for publication October 13, 2015.
Accepted for publication March 3, 2016.